JPE 16-3-30

http://dx.doi.org/10.6113/JPE.2016.16.3.1131
ISSN(Print): 1598-2092 / ISSN(Online): 2093-4718

A Novel Sliding Mode Observer for State of Charge Estimation of EV Lithium Batteries

Qiaoyan Chen†, Jiuchun Jiang*,**, Sijia Liu*,**, and Caiping Zhang*,**

†,*National Active Distribution Network Technology Research Center (NANTEC), School of Electrical Engineering, Beijing Jiaotong University, Beijing, China
†,**Collaborative Innovation Center of Electric Vehicles in Beijing, Beijing, China

Abstract

A simple design for a sliding mode observer is proposed for EV lithium battery SOC estimation in this paper. The proposed observer does not have the limiting conditions of existing observers. Compared to the design of previous sliding mode observers, the new observer does not require a solving matrix equation and it does not need many observers for all of the state components. As a result, it is simple in terms of calculations and convenient for engineering applications. The new observer is suitable for both time-variant and time-invariant models of battery SOC estimation, and the robustness of the new observer is proved by Liapunov stability theorem. Battery tests are performed with simulated FUDS cycles. The proposed observer is used for the SOC estimation on both unchanging parameter and changing parameter models. The estimation results show that the new observer is robust and that the estimation precision can be improved base on a more accurate battery model.

Key words: Lithium battery, Sliding mode observer, State estimation, State of charge

I. INTRODUCTION

Lithium batteries have many advantages such as high energy density, high power density, long cycle life and so on. They are widely used as the energy storage elements of electric vehicles. In order to improve the safety and reliability of a battery pack, fully play its efficiency, and prolong its life, the battery pack must be managed effectively. Battery state of charge (SOC) estimation is important since it is the basis of battery management systems (BMS). However, battery is a kind of nonlinear uncertain system. As a result, it is very difficult to accurately estimate battery SOC.

The common methods of SOC estimation are: 1. Current integration [1]: SOC is estimated by the time integral of the current with the initial SOC provided. However, the error increases with time. 2. Open circuit voltage (OCV) [2]: SOC is estimated based on the functional relationship between open circuit voltage and SOC. However, the battery must be set aside for a period of time. Unfortunately, this is not suitable for real-time SOC estimation. 3. Neural network [3]-[6]: a large number of samples with comprehensive data are required for model training and the sample data as well as the training methods affect the accuracy. 4. Kalman filter [4], [7]-[10]: SOC is estimated with algebraic iterative method. However, its accuracy is affected by model accuracy. 5. Predictive electromotive force (EMF) or OCV [11], [12]: these methods can estimate SOC accurately. However, the formulas involve many parameters, and the computation is complicated. 6. Mathematical fitting [13]: the function relationship SOC and the current, voltage, temperature and so on can be concluded by experiments. However, the function relationship is limited by the applicable conditions. 7. Impedance analysis [14]: SOC is estimated by battery electrochemical impedance spectroscopy analysis. However, this is only suitable for lab research.

Sliding mode observer is a kind of iterative algorithm which can be used in battery SOC estimation [15]-[20]. The design of previous sliding mode observers for battery SOC estimation includes: 1. Battery dynamic model is established in matrix form. Base on this model, an observer is designed which needs to solve the matrix equation. When the order of the matrix is relatively high, the calculations are more

Manuscript received Jul. 22, 2015; accepted Dec. 1, 2015
Recommended for publication by Associate Editor Jonghoon Kim.
†Corresponding Author: xychen@bjtu.edu.cn
Tel: +86-136-2113-2962, Beijing Jiaotong University
*National Active Distribution Network Technology Research Center, School of Electrical Engineering, Beijing Jiaotong University, China
**Collaborative Innovation Center of Electric Vehicles in Beijing, China

complicated [15], [16]. 2. Battery dynamic model is established in differential equations form. One observer is designed on the basis of each equation, which is needed to design multiple observers for all of the state components [17], [18]. Battery model parameters are changing in terms of some influence factors such as temperature, SOC, current rate and so on. Therefore, sometimes the model parameters are represented by variables which are functions of the above influence factors. The design method of the changing parameters system observer is the same as that for the above two methods [19], [20].

To improve methods for estimating battery SOC, this paper employs a novel sliding mode observer for SOC estimation. Firstly, based on battery Thevenin circuit model, taking the battery polarization voltage and open circuit voltage as state components, with the difference between the terminal voltage of the battery and the ohm resistance voltage drop as the observation, a two-dimensional state space equation is established to simplify the battery state equation. Secondly, based on the battery state equation, a novel observer, which does not possess the limiting condition of existing observers, is designed. The design of the new observer for SOC estimation does not need a solving matrix equation or multiple observers for all of the state components. Therefore, it can reduce the calculations in design and is easy to use in engineering.

The new observer can be used for both time-variant systems and time-invariant systems, and the observer design methods of the two kinds of systems are the same. The observer's robustness is proved by Lyapunov stability theorem. The characteristics of the new observer, based on the changing parameters model and the unchanging parameters model, are verified by tests. The verification shows that the new observer is robust and has a simple design. It also shows that improving the battery model accuracy can decrease the estimation error.

II. BATTERY MODELING

The Thevenin circuit model is shown in Fig. 1. It is simple and well simulated to the external features of batteries.

In Fig. 1, v_{oc} is the OCV, which is equal to the electromotive force of the battery; r_0 is the ohm internal resistance of the battery; c_1 and r_1 are polarization capacitance and resistance; v_t is terminal voltage of the battery; v_1 is the polarized voltage; and i_t is the input current. The results are as follows:

$$\dot{v}_1 c_1 + \frac{v_1}{r_1} = i_t \tag{1}$$

Therefore, the differential equation of v_1 is:

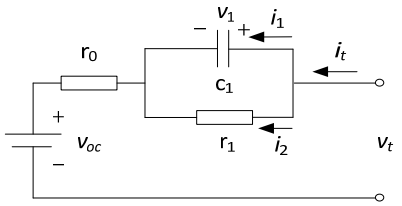

Fig. 1. Battery Thevenin model.

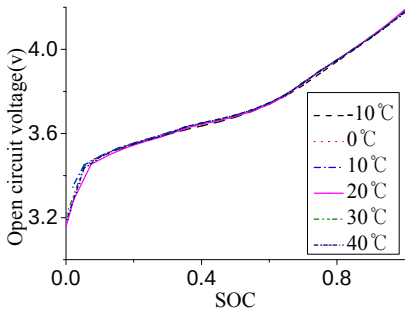

Fig. 2. OCV vs. SOC at different temperatures.

$$\dot{v}_1 = -\frac{1}{r_1 c_1} v_1 + \frac{1}{c_1} i_t \tag{2}$$

There exist a function relationship $v_{oc} = g(S_{oc})$ between OCV and SOC, where S_{oc} represents SOC, and the function does not experience a significant change with temperature [17], [18], [21]. The test battery OCV vs. SOC curves at -10℃, 0℃, 10℃, 20℃, 30℃ and 40℃ are shown in Fig. 2. From Fig. 2, it can be seen that the test battery OCV curves have small differences. In addition, the battery test was operated in thermostat. Therefore, this paper take it as an invariant function. As a result, the differential equation with t as the time is:

$$\dot{v}_{oc} = \frac{dg(S_{oc})}{dS_{oc}} \cdot \dot{S}_{oc} = k\dot{S}_{oc} = k\frac{\eta i_t}{Q_n} \tag{3}$$

In equation (3), k is the derived function of the OCV with respect to the SOC and it is changed with the SOC accordingly; η is the discharge efficiency as well as a variable; and Q_n is the battery capacity. Based on equations (2) and (3), the battery model is:

$$\dot{v}_1 = -\frac{1}{r_1 c_1} v_1 + \frac{1}{c_1} i_t + f_1 \tag{4}$$

$$\dot{v}_{oc} = \frac{i_t}{Q_n} + f_2 \tag{5}$$

Equation (5) is the result of k and η in (3) after being substituted with 1, the error is merged into the rear nonlinear uncertain function. The two bounded functions f_1 and f_2 are the error-sum of linearization, noise and other factors. In line with the current direction in Fig. 1, the system terminal voltage is:

$$v_t = v_{oc} + i_t r_0 + v_1 \tag{6}$$

Since the terminal voltage v_t, current i_t and ohm internal resistance r_0 can be obtained by measurement, it is possible

to choose $v_y = v_t - i_t r_0$ as an observation. Then the observation equation is:

$$v_y = v_{oc} + v_1 \tag{7}$$

Equations (4), (5) and (7) are battery state space equations where the state variable is $\boldsymbol{x} = [v_1, v_{oc}]^{\mathrm{T}}$, the observation is $\boldsymbol{y} = v_y$, and the input is $\boldsymbol{u} = i_t$. Therefore, the coefficient matrices are: $\boldsymbol{A} = \begin{bmatrix} -\frac{1}{r_1 c_1} & 0 \\ 0 & 0 \end{bmatrix}$, $\boldsymbol{B} = \left[\frac{1}{c_1}, \frac{1}{Q_n}\right]^{\mathrm{T}}$, $\boldsymbol{C} = [1 \quad 1]$.

The system state is estimated with a sliding mode observer which needs the system's linear part to be observable. Based on the necessary and sufficient condition, the result is as follows:

$$\mathrm{rank}\boldsymbol{H} = \mathrm{rank}[\boldsymbol{C}^{\mathrm{T}} \quad \boldsymbol{C}\boldsymbol{A}^{\mathrm{T}}] = \mathrm{rank}\begin{bmatrix} 1 & 1 \\ -\frac{1}{r_1 c_1} & 0 \end{bmatrix} \tag{8}$$

Since $-\frac{1}{r_1 c_1} \neq 0$, $\mathrm{rank}\boldsymbol{H} = 2$. Then the linear part of the battery state equation is observable.

The relationship between the SOC as an independent variable and the OCV as a function is shown in Fig. 2. If the OCV is an independent variable and the SOC is a function, the result at 20℃ is shown in Fig. 3. The OCV can be estimated by the sliding mode observer. Based on the relationship between the SOC and the OCV $S_{oc} = g^{-1}(v_{oc})$, the SOC can be estimated with the OCV as an independent variable and the SOC as a function.

In applications, it is possible to obtain the battery state components polarization voltage and the OCV by algebraic iteration of the novel sliding mode observer. The SOC is estimated based on the function relationship between the OCV and the SOC. The SOC can be estimated in real-time by the novel observer, which meets the demands of electric vehicles.

III. THE NOVEL SLIDING MODE OBSERVER METHOD FOR SOC ESTIMATION

A. Underlying Theory

The following is a kind of nonlinear uncertain system:

$$\dot{\boldsymbol{x}}(t) = \boldsymbol{A}\boldsymbol{x}(t) + \boldsymbol{B}\boldsymbol{u}(t) + \boldsymbol{f}(\boldsymbol{x}, \boldsymbol{u}, t) \tag{9}$$

$$\boldsymbol{y}(t) = \boldsymbol{C}\boldsymbol{x}(t) \tag{10}$$

Where $\boldsymbol{A} \in R^{n\times n}$, $\boldsymbol{B} \in R^{n\times \mathrm{m}}$, $\boldsymbol{C} \in R^{l\times n}$, $n \geq l \geq m$ and $u(t) \in R^{\mathrm{m}}$ is known system control variables, with full-rank $\boldsymbol{B}$, $\boldsymbol{C}$, observable $(\boldsymbol{A}, \boldsymbol{C})$,as well as bounded, nonlinear, and uncertain function $\boldsymbol{f}(\boldsymbol{x}, \boldsymbol{u}, t) = [f_1, f_1, \ldots, f_n]^{\mathrm{T}} \in R^n$. The existing sliding mode observer for the system must satisfy $\boldsymbol{f}(\boldsymbol{x}, \boldsymbol{u}, t) = \boldsymbol{B}\boldsymbol{\xi}(\boldsymbol{x}, \boldsymbol{u}, t)$, where $\boldsymbol{\xi}(\boldsymbol{x}, \boldsymbol{u}, t) \in R^m$ is an arbitrary bounded function. Compared with the existing observers, the novel observer, which does not have the limiting condition above, is proposed for SOC estimation in this paper.

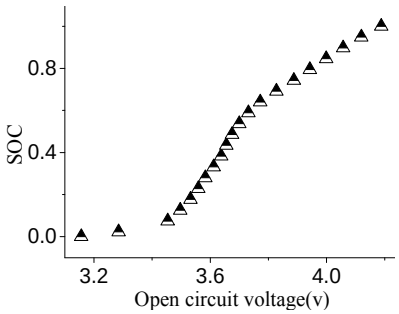

Fig. 3. SOC vs. OCV at 20℃.

For equations (9) and (10), the design of the new observer is as follows [22], [23]:

$$\dot{\hat{\boldsymbol{x}}}(t) = \boldsymbol{A}\hat{\boldsymbol{x}}(t) + \boldsymbol{B}\boldsymbol{u}(t) - \boldsymbol{G}(\boldsymbol{C}\hat{\boldsymbol{x}}(t) - \boldsymbol{y}(t)) + \boldsymbol{B}\boldsymbol{v} \tag{11}$$

$\hat{\boldsymbol{x}}(t) \in R^{\mathrm{n}}$ is the system state vector estimation, $\boldsymbol{G} \in R^{n\times l}$ is the designed matrix, and $\boldsymbol{v}(t) \in R^{\mathrm{n}} \times R^{+} \to R^{\mathrm{n}}$ is the control variable designed for the observer. If the error of the system state vector estimation is $\boldsymbol{e}(t) = \hat{\boldsymbol{x}}(t) - \boldsymbol{x}$, the design for the sliding mode surface is as follows:

$$\boldsymbol{S} = \boldsymbol{F}(\hat{\boldsymbol{y}}(t) - \boldsymbol{y}(t)) = \boldsymbol{F}\boldsymbol{C}(\hat{\boldsymbol{x}}(t) - \boldsymbol{x}(t)) = \boldsymbol{M}\boldsymbol{e} = 0 \tag{12}$$

Where $\hat{\boldsymbol{y}}(t) \in R^{l}$ is the system observation estimation, $\boldsymbol{F}$ is the designed matrix, which makes the state variables in the surface slid to the zero equilibrium point, and $\boldsymbol{M} = \boldsymbol{F}\boldsymbol{C}$. The control variable $\boldsymbol{v}$ is designed as [22], [23]:

$$\boldsymbol{v} = \begin{cases} -\dfrac{(\boldsymbol{S}^{\mathrm{T}}\boldsymbol{M}\boldsymbol{B})^{\mathrm{T}}}{\left\|\boldsymbol{S}^{\mathrm{T}}\boldsymbol{M}\boldsymbol{B}\right\|^2}(\nabla_1 + \nabla_2) & \left\|\boldsymbol{S}^{\mathrm{T}}\boldsymbol{M}\boldsymbol{B}\right\| \neq 0 \\ 0 & \left\|\boldsymbol{S}^{\mathrm{T}}\boldsymbol{M}\boldsymbol{B}\right\| = 0 \end{cases} \tag{13}$$

Where $\nabla_1 = \rho\|\boldsymbol{S}\|\|\boldsymbol{M}\boldsymbol{B}\|$, $\nabla_2 = \eta(\frac{1}{2})^{\beta}\|\boldsymbol{S}\|^{2\beta}$, $\beta \geq 0$, and $0 \geq \eta \geq 1$.

Based on equations (9) and (11), the following equation for the estimation error is:

$$\dot{\boldsymbol{e}}(t) = \boldsymbol{A}_0\boldsymbol{e}(t) - \boldsymbol{f}(\boldsymbol{x}, \boldsymbol{u}, t) + \boldsymbol{B}\boldsymbol{v} \tag{14}$$

Where $\boldsymbol{A}_0 = \boldsymbol{A} - \boldsymbol{G}\boldsymbol{C}$. If the error is partitioned as $\boldsymbol{e} = [\boldsymbol{e}_1; \boldsymbol{e}_2]$ with $\boldsymbol{e}_1 \in R^{\mathrm{n-m}}$ and $\boldsymbol{e}_2 \in R^{\mathrm{m}}$, the error state equations in partitioned matrix form are as follows:

$$\dot{\boldsymbol{e}}_1(t) = \boldsymbol{A}_{011}\boldsymbol{e}_1(t) + \boldsymbol{A}_{012}\boldsymbol{e}_2(t) + \boldsymbol{f}_1 + \boldsymbol{B}_1\boldsymbol{v} \tag{15}$$

$$\dot{\boldsymbol{e}}_2(t) = \boldsymbol{A}_{021}\boldsymbol{e}_1(t) + \boldsymbol{A}_{022}\boldsymbol{e}_2(t) + \boldsymbol{f}_2 + \boldsymbol{B}_2\boldsymbol{v} \tag{16}$$

Accordingly, the sliding mode surface in partitioned matrix form is as follows:

$$\boldsymbol{S} = \boldsymbol{M}\boldsymbol{e} = \boldsymbol{M}_1\boldsymbol{e}_1 + \boldsymbol{M}_2\boldsymbol{e}_2 = 0 \tag{17}$$

In the above expressions, $\boldsymbol{M} \in R^{n\times n}$, $\boldsymbol{M} = [\boldsymbol{M}_1, \boldsymbol{M}_2]$, $\boldsymbol{M}_1 \in R^{n\times(n-m)}$, $\boldsymbol{M}_2 \in R^{n\times m}$, $\boldsymbol{A}_{011}$, $\boldsymbol{A}_{012}$, $\boldsymbol{A}_{021}$, and $\boldsymbol{A}_{022}$ are partitions of $\boldsymbol{A}_0$, $\boldsymbol{A}_{011} \in R^{(n-m)\times(n-m)}$, $\boldsymbol{A}_{012} \in R^{(n-m)\times m}$, $\boldsymbol{A}_{021} \in R^{m\times(n-m)}$, $\boldsymbol{A}_{022} \in R^{m\times m}$, $\boldsymbol{B} = [\boldsymbol{B}_1; \boldsymbol{B}_2]$, $\boldsymbol{B}_1 \in R^{(n-m)\times m}$, $\boldsymbol{B}_2 \in R^{m\times m}$, $\boldsymbol{f} = [\boldsymbol{f}_1; \boldsymbol{f}_2]$, $\boldsymbol{f}_1 \in R^{n-m}$, and $\boldsymbol{f}_2 \in R^{m}$.

For the error components are not linear correlation, the linear transformation in the error system will not change the convergence of the error system. Therefore, the error system

(15), (16) and the sliding mode surface in the partitions form (17) can be transformed as:

$$\dot{\boldsymbol{e}}_1'(\boldsymbol{t}) = \boldsymbol{A}_{011}'\boldsymbol{e}_1'(\boldsymbol{t}) + \boldsymbol{A}_{012}'\boldsymbol{e}_2'(\boldsymbol{t}) + \boldsymbol{B}_1'\boldsymbol{v} \quad (18)$$

$$\dot{\boldsymbol{e}}_2'(\boldsymbol{t}) = \boldsymbol{A}_{021}'\boldsymbol{e}_1'(\boldsymbol{t}) + \boldsymbol{A}_{022}'\boldsymbol{e}_2'(\boldsymbol{t}) + \boldsymbol{f}_2' + \boldsymbol{B}_2'\boldsymbol{v} \quad (19)$$

$$\boldsymbol{S}' = \boldsymbol{M}'\boldsymbol{e}' = \boldsymbol{M}_1'\boldsymbol{e}_1' + \boldsymbol{M}_2'\boldsymbol{e}_2' = 0 \quad (20)$$

The designed observer shows robustness against modeling errors, when the following three assumptions for the sliding mode observer (11)-(13) are satisfied.

A1: Let

$$\boldsymbol{A}_S = \boldsymbol{M}^{\mathrm{T}}\boldsymbol{M}\boldsymbol{A}_0 \quad (21)$$

For the sliding mode observer (11)-(13), the matrixes $\boldsymbol{M}$ and $\boldsymbol{G}$ are designed to make $\boldsymbol{A}_0$ satisfy $\lambda_{\max}(\boldsymbol{A}_0) \le 0$ and to make $\boldsymbol{A}_S$ satisfy $\lambda_{\max}(\boldsymbol{A}_S) \le 0$, where $\lambda_{\max}(\boldsymbol{A}_0)$ and $\lambda_{\max}(\boldsymbol{A}_S)$ are the matrix maximum eigenvalues of $\boldsymbol{A}_0$ and $\boldsymbol{A}_S$, respectively.

A2: In equation (13), parameter ρ is satisfied by $\rho\|\boldsymbol{MB}\| \ge \|\boldsymbol{Mf}\|$.

Satisfy assumptions A1 and A2, and the control variable (13) can make the system state vector $\boldsymbol{x(t)}$ move to the sliding mode surface (12).

A3: Let:

$$\boldsymbol{A}_M = \boldsymbol{A}_{011}' - \boldsymbol{A}_{012}'\boldsymbol{M}_2'^{-1}\boldsymbol{M}' \quad (22)$$

The matrix $\boldsymbol{M}'$ is designed to make $\boldsymbol{A}_M$ the same as a Hurwitz matrix, and the sliding mode observer can make the error vector converge to an equilibrium point $\boldsymbol{e(t)=0}$.

B. Verifying the Robustness of the Novel Sliding Mode Observer

The following is to verify the robustness of the novel sliding mode observer (11)-(13) against the nonlinear functions $\boldsymbol{f(x,u,t)}$ in system (9) and (10).

Take the Lyapunov function as:

$$V = \frac{1}{2}\boldsymbol{S}^{\mathrm{T}}\dot{\boldsymbol{S}} = \frac{1}{2}\|\boldsymbol{S}\|^2 \ge 0 \quad (23)$$

The derivative is as follows with *t* as the time:

$$\begin{aligned}\dot{V} = \boldsymbol{S}^{\mathrm{T}}\dot{\boldsymbol{S}} &= \boldsymbol{e}^{\mathrm{T}}\boldsymbol{M}^{\mathrm{T}}\boldsymbol{M}\dot{\boldsymbol{e}} = \boldsymbol{e}^{\mathrm{T}}\boldsymbol{M}^{\mathrm{T}}\boldsymbol{M}(\boldsymbol{A}_0\boldsymbol{e} - \boldsymbol{f} + \boldsymbol{B}\boldsymbol{v}) \\ &= \boldsymbol{e}^{\mathrm{T}}\boldsymbol{M}^{\mathrm{T}}\boldsymbol{M}\boldsymbol{A}_0\boldsymbol{e} - \boldsymbol{S}^{\mathrm{T}}\boldsymbol{M}\boldsymbol{f} + \boldsymbol{S}^{\mathrm{T}}\boldsymbol{M}\boldsymbol{B}\boldsymbol{v} \\ &\le \lambda_{\max}(\boldsymbol{A}_S)\|\boldsymbol{e}\|^2 - \boldsymbol{S}^{\mathrm{T}}\boldsymbol{M}\boldsymbol{f} + \boldsymbol{S}^{\mathrm{T}}\boldsymbol{M}\boldsymbol{B}\boldsymbol{v} \\ &\le \|\boldsymbol{S}\|\|\boldsymbol{M}\boldsymbol{f}\| + \boldsymbol{S}^{\mathrm{T}}\boldsymbol{M}\boldsymbol{B}\boldsymbol{v} \\ &= \|\boldsymbol{S}\|\|\boldsymbol{M}\boldsymbol{f}\| - (\rho\|\boldsymbol{S}\|\|\boldsymbol{M}\boldsymbol{B}\| + \eta(\tfrac{1}{2})^{\beta}\|\boldsymbol{S}\|^{2\beta})\end{aligned}$$

If the parameter is $\rho\|\boldsymbol{MB}\| \ge \|\boldsymbol{Mf}\|$ and $\boldsymbol{S} \ne 0$, then:

$$\dot{V} \le -\eta(\tfrac{1}{2})^{\beta}\|\boldsymbol{S}\|^{2\beta} < 0 \quad (24)$$

Now the state vectors will converge to the sliding mode surface. When the vector reaches the surface, it will slide along the surface accompanied by up and down quivering. The expression of the sliding mode surface (20) shows: $\boldsymbol{M}_1'\boldsymbol{e}_1' = -\boldsymbol{M}_2'\boldsymbol{e}_2'$. Therefore, $\boldsymbol{e}_2' = -\boldsymbol{M}_2'^{-1}\boldsymbol{M}_1'\boldsymbol{e}_1'$, if it is substituted into equation (18), and equations (12) and (13) can tell that $\boldsymbol{v} = 0$ on the sliding mode surface. Finally, it can be known that the dynamic feature of the error state vector on the sliding mode surface is:

$$\dot{\boldsymbol{e}}_1'(\boldsymbol{t}) = (\boldsymbol{A}_{011}' - \boldsymbol{A}_{012}'\boldsymbol{M}_2'^{-1}\boldsymbol{M}_1')\boldsymbol{e}_1'(\boldsymbol{t}) = \boldsymbol{A}_M\boldsymbol{e}_1'(\boldsymbol{t}) \quad (25)$$

If $\boldsymbol{A}_M$ is a Hurwitz matrix, the error state will be converged to an equilibrium point $\boldsymbol{e(t)=0}$. Therefore, the sliding mode observer is stable. The speed of the convergence will be affected by the eigenvalue of $\boldsymbol{A}_M$.

The proving processes are suitable for both time-varying systems and time-invariant systems. Therefore, the new observer method can be used in the two systems. The design methods for the time-invariant system observer and the time-varying system observer are the same. Battery model parameters are functions of temperature, current rate, SOC and so on, and the functions can be obtained by testing.

C. Sliding Mode Observer Design

The design procedures of the new sliding mode observer method for SOC estimation are as follows:

D1. According to the error state function (14), the matrix function $\boldsymbol{A}_0 = \boldsymbol{A} - \boldsymbol{GC}$ is known. The matrix is designed so that $\boldsymbol{G} = 0$. Then $\boldsymbol{A}_0 = \boldsymbol{A} = \begin{bmatrix} -1/r_1c_1 & 0 \\ 0 & 0 \end{bmatrix}$. As a result, $\lambda_{\max}(\boldsymbol{A}_0) \le 0$. The matrix was designed so that $\boldsymbol{F} = 1$. Then $\boldsymbol{M} = \boldsymbol{FC} = [1 \quad 1]$. According to equation (21) $\boldsymbol{A}_S = 2\boldsymbol{A}_0$. Therefore, $\lambda_{\max}(\boldsymbol{A}_S) \le 0$.

D2. The following parameter was designed so that $\rho = 10$, which makes $\rho\|\boldsymbol{MB}\| \ge \|\boldsymbol{Mf}\|$ in this test.

D3. Meanwhile, $\boldsymbol{A}_{012} = \boldsymbol{A}_{021} = \boldsymbol{A}_{022} = 0$, and the coefficient matrices of the error equation (18) is $\boldsymbol{A}_{011}' = -1/r_1c_1$, $\boldsymbol{A}_{012}' = 0$. According to expression (22) $\boldsymbol{A}_M = \boldsymbol{A}_{011}'$, which is a Hurwitz matrix.

The observer estimators are OCV v_{oc} and the polarization voltage v_1. In addition, the whole algorithm estimator is the SOC. For the test in this paper, the designed parameters values of the new observer are shown in Table I.

The three assumptions mentioned in previous are satisfied according to the above designs. Therefore, the new observer is robust to the uncertain part $\boldsymbol{f(x,u,t)}$ in the model. The discrete form of the new observer is:

$$\begin{cases} \hat{\boldsymbol{y}}(\boldsymbol{k}) = \boldsymbol{C}\hat{\boldsymbol{x}}(\boldsymbol{k}); \quad \boldsymbol{M} = \boldsymbol{FC} \\ \boldsymbol{S}(\boldsymbol{k}) = \boldsymbol{M}(\hat{\boldsymbol{x}}(\boldsymbol{k}) - \boldsymbol{x}(\boldsymbol{k})) = \boldsymbol{F}(\hat{\boldsymbol{y}}(\boldsymbol{k}) - \boldsymbol{y}(\boldsymbol{k})) \\ \boldsymbol{v}(\boldsymbol{k}) = \begin{cases} -\dfrac{(\boldsymbol{S}(\boldsymbol{k})^{\mathrm{T}}\boldsymbol{MB})^{\mathrm{T}}}{\|\boldsymbol{S}(\boldsymbol{k})^{\mathrm{T}}\boldsymbol{MB}\|^2}(\nabla_1(\boldsymbol{k}) + \nabla_2(\boldsymbol{k})) & \|\boldsymbol{S}(\boldsymbol{k})^{\mathrm{T}}\boldsymbol{MB}\| \ne 0 \\ 0 & \|\boldsymbol{S}(\boldsymbol{k})^{\mathrm{T}}\boldsymbol{MB}\| = 0 \end{cases} \\ \mathrm{d}\hat{\boldsymbol{x}}(\boldsymbol{k}) = \boldsymbol{A}\hat{\boldsymbol{x}}(\boldsymbol{k}) + \boldsymbol{B}\boldsymbol{u}(\boldsymbol{k}) - \boldsymbol{G}(\boldsymbol{C}\hat{\boldsymbol{x}}(\boldsymbol{k}) - \boldsymbol{y}(\boldsymbol{k})) + \boldsymbol{B}\boldsymbol{v}(\boldsymbol{k}) \end{cases} \quad (26)$$

TABLE I
THE DESIGNED PARAMETERS VALUES

parameters	G	F	ρ	β	η
values	0	1	10	1	0.95

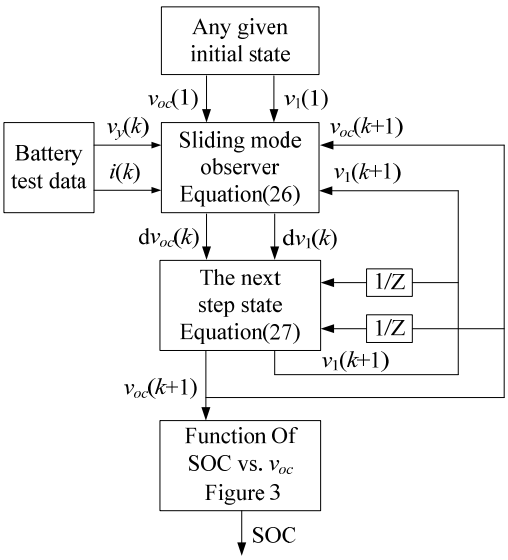

Fig. 4. The whole SOC estimation algorithm.

Where $\nabla_1 = \rho\|\boldsymbol{S(k)}\|\|\boldsymbol{MB}\|$ and $\nabla_2 = \eta(\frac{1}{2})^{\beta}\|\boldsymbol{S(k)}\|^{2\beta}$.

$$\hat{\boldsymbol{x}}(\boldsymbol{k}+1) = \hat{\boldsymbol{x}}(\boldsymbol{k}) + \mathrm{d}\hat{\boldsymbol{x}}(\boldsymbol{k}) \cdot \Delta t \tag{27}$$

Where the sampling period $\Delta t = 1\mathrm{s}$. Taking the coefficients of equations (4), (5) and (7) and the designed parameters values into the discrete form of the observer equations (26) and (27), the OCV as the system state vector component can be estimated by iterative computation, and the SOC can be estimated by the function of SOC vs. OCV. The overall SOC estimation algorithm is shown in Fig. 4.

For the design of the exiting slide mode observer it is necessary to solve the matrix equation or to design multiple observers for all of the state components, and the design calculation is complex. Through its design processes, the new observer does not need to solve the matrix equation or design many observers. Therefore, it is simple and convenient for engineering applications.

IV. SOC ESTIMATION BY THE NEW OBSERVER METHOD

To verify the performance of the novel sliding mode observer method for battery SOC estimation, a test under preset conditions for a lithium battery is operated, in which the SOC estimation and the ideal value are compared. The test battery shown in Fig. 5 is a 25Ah Lithium power battery.

The testing platform consists of the Arbin BT2000 battery tester for discharging and charging batteries shown in Fig. 6, the incubator shown in Fig. 7, a host computer and

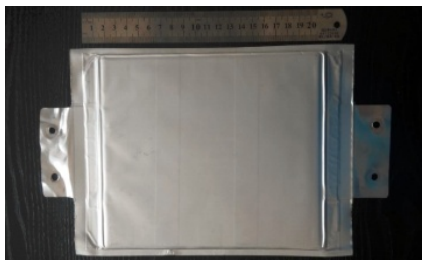

Fig. 5. The test battery.

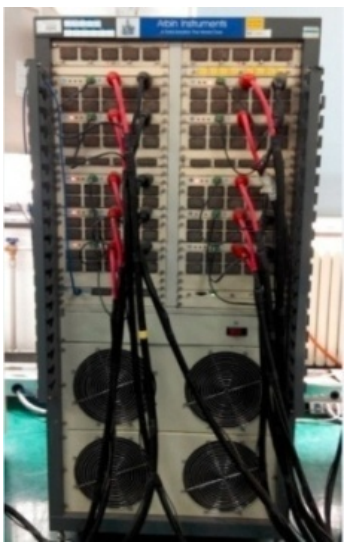

Fig. 6. Arbin BT2000 battery test equipment.

Fig. 7. Incubator.

monitoring software for the working processes. The monitoring software of the host computer can set the battery state while monitoring and collecting information on the current, voltage and temperature. The incubator can guarantee a set temperature for the battery.

A. Battery Circuit Model Parameter Extraction

Extracting the parameters of Thevenin circuit model is necessary when using the new sliding mode observer method for SOC estimation. In this case the pulse current is used for

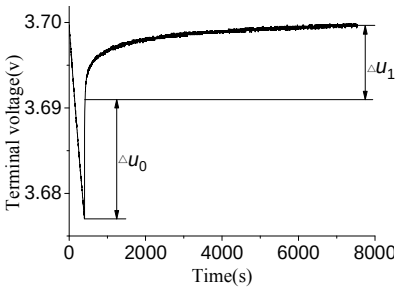

Fig. 8. Battery terminal voltage after pulse current.

the extraction. At room temperature, the pulse current become 0A suddenly from the C/3 discharge rate, and the battery terminal voltage change curve at SOC=0.537 is shown in Fig. 8.

From Fig. 1, it can be seen that the ohm internal resistance of the battery Thevenin model is $r_0 = \Delta u_0 / i$, and that the polarization internal resistance is $r_1 = \Delta u_1 / i$.

According to the dynamic feature of the RC circuit, the time constant is $\tau = r_1 c_1$. After the current pulse discharging for τ, the battery terminal voltage increases to $63.2\% \Delta u_1$.

The model parameters can be computed based on the above expression, and the terminal voltage curve of the battery after a pulse is shown in Fig. 8. The results of the model parameters at SOC=0.537 are: $r_0 = 1.24\text{m}\Omega$, $r_1 = 1.46\text{m}\Omega$ and $c_1 = 1.24 \times 10^5 \text{F}$.

B. Simulation FUDS Condition Estimation Result

The performance of the new sliding mode observer will be verified under the simulated FUDS condition with the battery shown in Fig. 5. The test is designed as follows: At room temperature, a battery with an initial SOC of 100% is selected. The simulated FUDS condition includes discharge and charge processes. To prevent the battery from being over charged, 1AH is discharged at the C/3 rate. Then the battery is run under the simulated FUDS condition set by the host computer, and stopped the test when the battery terminal voltage reaches 3v. At this point, the SOC may not be 0. The current and the terminal voltage under the simulated FUDS condition are shown in Fig. 9.

The battery SOC is estimated with a new observer under the simulation FUDS condition, during which the initial value of the open circuit voltage can be set randomly within the stable range of the observer. If the initial polarized voltage $v_1 = 0$ and the initial open circuit voltage is 3v, then $\boldsymbol{x_0} = [0;3]$. After iterative computation, the estimated values and the measured values of the observation are shown in Fig. 10.

From Fig. 10, it can be seen that the estimated observation converges to the measured observation rapidly in the initial stage, after stabilization, the estimated values shake up and down along with the measured values. If the initial states are

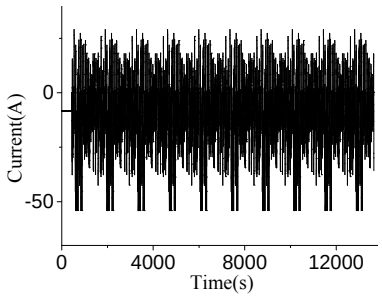

(a) Battery current.

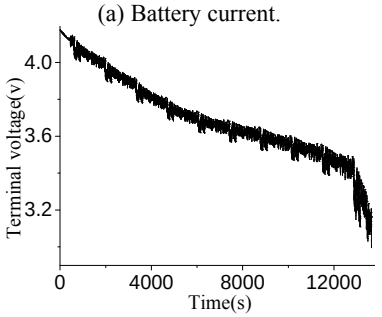

(b) Battery terminal voltage.

Fig. 9. Discharge current and terminal voltage.

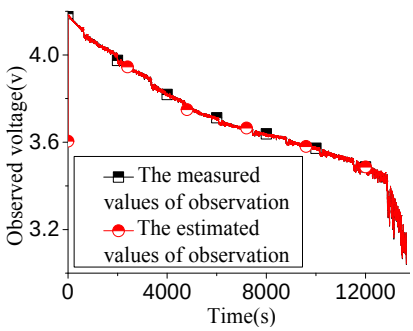

(a) The two observations.

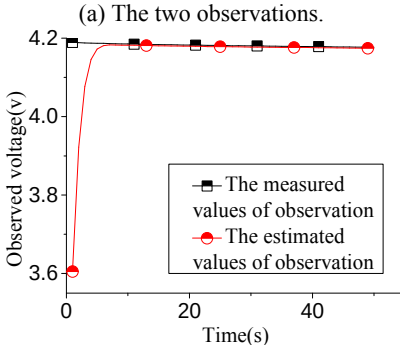

(b) The two observations in 1st-50th s.

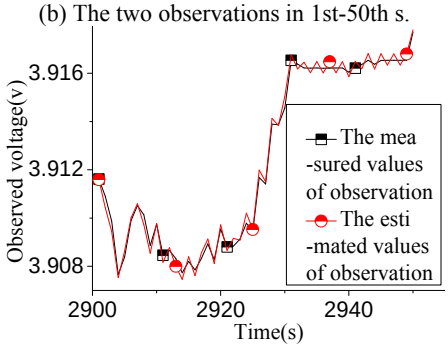

(c) The two observations in 2901st-2950th s.

Fig. 10. The estimated values and the measured values of the observation.

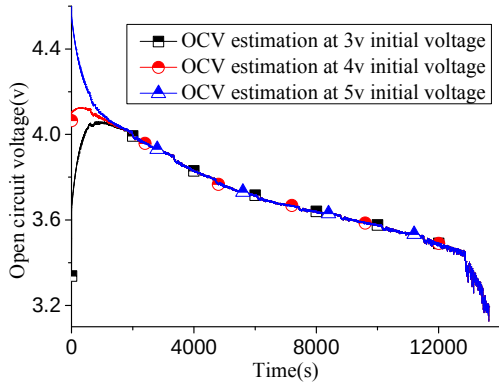

Fig. 11. Battery OCV estimation by the new sliding mode observer.

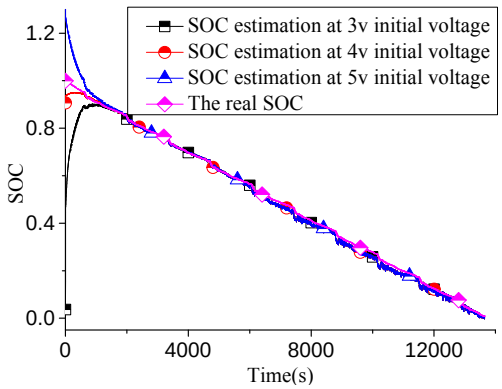

Fig. 12. Battery SOC estimation.

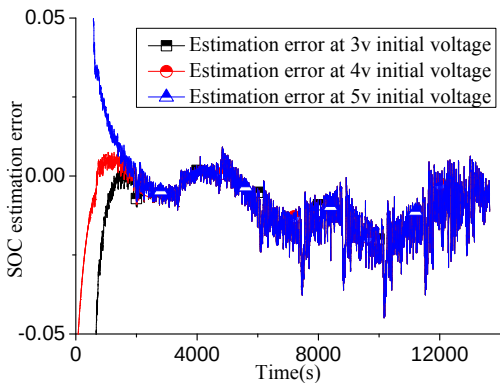

Fig. 13. Battery SOC estimation error.

set like the other values, similar results can be obtained.

The initial value of the polarized voltage is $v_1 = 0$, and the initial values of the open circuit voltage v_{oc} are 3v, 4v and 5v. After the iterative computation, the open circuit voltage estimation results are shown in Fig. 11. They have almost equal convergent results.

The SOC can be estimated based on the relationship between the OCV and the SOC in Fig. 3. Under the simulated FUDS condition, the battery discharge efficiency is $\eta \neq 1$. After the test and a rest for 2 hours, the OCV changed to 3.2216v. As a result, the SOC is 0.0079 instead of 0, with 0.2122AH left. The sum of the discharge coulomb, counted

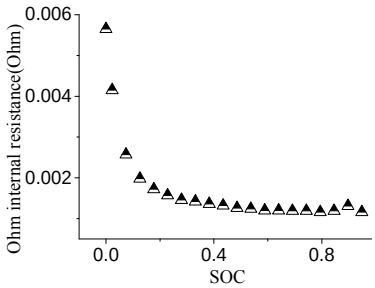

Fig. 14. The relationship between ohm internal resistance and SOC.

by the discharging efficiency $\eta = 1$, and the remaining capacity is almost the full capacity of the battery. Therefore, the average discharging efficiency is set as 1. The real SOC can be computed with the current integration method since the initial SOC is 100%. The estimated SOC and the real value are shown in Fig. 12 and the estimation error is shown in Fig. 13.

Fig. 12 shows that the SOC estimation by the new sliding mode observer method converges to the ideal value under simulation FUDS condition in spite of different initial open circuit voltages.

Fig. 13 shows the corresponding SOC estimation error. After stabilization, when the initial voltage is set to 3v, 4v and 5v, the estimation errors are all within 4.5%. Likewise, similar results can be obtained when the initial state, which is in the stable range of the observer, is set to different values. Test analysis shows that the estimation results are not affected by the initial values, which are within the stable range. The test with the simulated FUDS condition shows that the new sliding mode observer method is robust to nonlinear uncertain systems.

C. Changing Parameters Model Estimation Result

Battery is a kind of complex time-varying system, and many influence factors, such as SOC, current rate, temperature and so on, can cause changes in the model parameters, which affects the SOC estimation. The function relationships between the parameters and influence factors can be obtained by testing.

Battery is a kind of complicated nonlinear uncertain system. Therefore, the design guidelines of the new observer consider the parameters changes which effect the SOC estimation, and some of the major factors that influence parameters changes. In the new observer, r_0 has a significant influence on the SOC estimation. r_0 changes with the above influence factors, and the function $r_0 = r_0(S_{oc}, i, T)$ can be concluded by testing, where T is the battery temperature. In the test, the battery was operated in thermostat, and the current rate was not more than 2C. Therefore, the effects of the current rate and temperature were not considered. The battery SOC was changed from

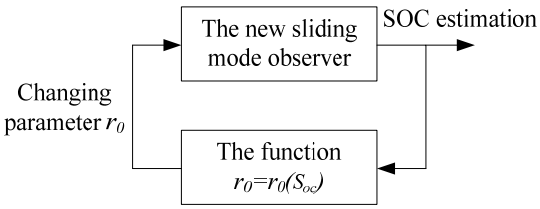

Fig. 15. Circulation iterative algorithm of the new observer.

TABLE II
BATTERY TIME-VARYING SYSTEM MODEL PARAMETERS

parameters	$r_0(m\Omega)$	$r_1(m\Omega)$	$c_1(F)$	$Q_n(C)$
values	$r_0(S_{oc})$	1.46	1.22×10^5	9.66×10^4

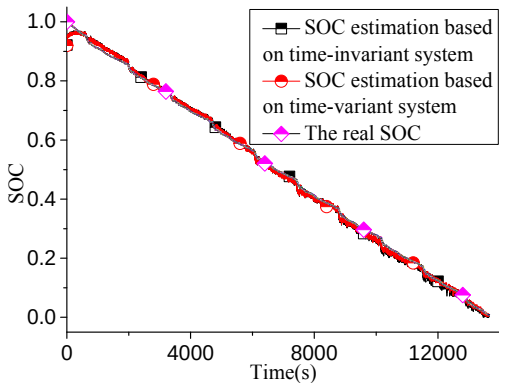

Fig. 16. SOC estimation based on time-invariant model and time-variant model.

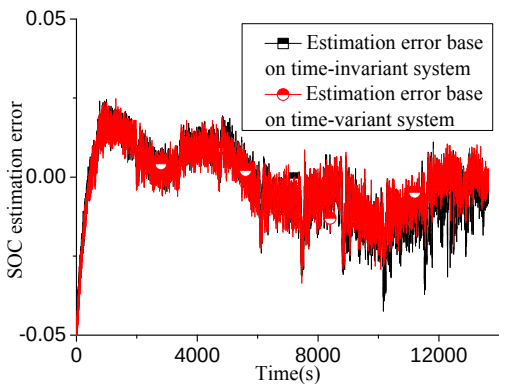

Fig. 17. SOC estimation error base on time-invariant and time-variant systems.

100% to 0%, and the function $r_0 = r_0(S_{oc})$ is shown in Fig. 14. It can be seen from Fig. 14 that r_0 is increased greatly when the SOC decreases form 100% to 0%. Therefore, the model parameter $r_0 = r_0(S_{oc})$ is chosen in this paper.

The verifying processes show that the new observer is suitable for both time-varying systems and time-invariant systems. The function $r_0 = r_0(S_{oc})$ is substituted in the system equation, and the changing parameter $r_0(S_{oc})$ is used in the new observer for the SOC estimation, which is a circulation iterative approach algorithm [19], [20]. The algorithm schematic diagram is shown in Fig. 15. The observer design methods of the two systems are the same [19], [20].

The analysis shows, that when the design parameters of the time-varying battery system applied to the hardware experiment are same as those in Table I, the new observer is robust. According to the identified model parameters above, the time-varying battery system model parameters are shown in Table II.

Similarly, the OCV is the observer estimator, and the SOC is the whole algorithm estimator. By taking the designed parameters and the model parameters into functions (26) and (27), the OCV can be obtained.

Let the initial state $\boldsymbol{x}_0 = [0;4]$. The SOC estimation of the hardware realization is based on both the changing and unchanging parameter models, which are shown in Fig. 16, and the estimation error is shown in Fig. 17.

From Figs. 16 and 17, it can be seen that updating parameters in real time can improve the accuracy of the estimation. Similar results can be obtained if the initial open circuit voltage is 3v and 5v. When the initial voltage is set as 3v, 4v and 5v, the maximum estimation errors are about 3.4%.

A battery is a strongly nonlinear uncertain system. Therefore, it is very difficult to accurately establish battery model. The SOC estimation used the new observer is on the basis of the battery model, and it is worth further study in terms of establishing a more precise battery model to improve estimation accuracy. The battery model, measuring accuracy, battery nonlinear characteristics and other characteristics contributed to estimation errors. In order to further decrease estimation errors, it is necessary to improve the precision of measurement, battery performance and so on.

V. CONCLUSION

(1) A novel sliding mode observer was proposed in this paper. It was developed from existing observers, for battery SOC estimation. Through the design of the new sliding mode observer, it can be seen that it is simpler than the existing observer design method and convenient for engineering applications.

(2) The robustness of the new observer is verified by Liapunov stability theory and simulation FUDS condition testing.

(3) The new observer can be used for both changing and unchanging parameters model SOC estimations, and the observer design methods are the same. Through tests, it can be seen that the estimation accuracy is improved when the model parameters are updated in real-time.

(4) In order to improve estimation precision, there needs to be further study on battery performance. In addition, more accurate models need to be established in future research.

ACKNOWLEDGMENT

The work was supported by the National Natural Science Foundation of China (No. 51277010).

REFERENCES

[1] K. S. Ng, C. Moo, Y.-P. Chen, and Y.-C. Hsieh, "Enhanced coulomb counting method for estimating state-of-charge and state-of-health of lithium-ion batteries," *Applied Energy*, Vol. 86, No. 9, pp. 1506-1511, Sep. 2009.

[2] J. H, Aylor, A. Thieme, and B. W. Johnson, "A battery state of charge indicator for electric wheelchairs," *IEEE Trans. Ind. Electron.*, Vol. 39, No. 5, pp. 398-409, Oct. 1992.

[3] B. Cheng, Z. Bai, and B. Cao, "State of charge estimation based on evolutionary neural network," *Energy Conversion and Management*, Vol. 49, No. 10, pp. 2788–2794, Oct. 2008.

[4] M. Charkhgard and M. Farrokhi, "State-of-charge estimation for lithium-ion batteries using neural networks and EKF," *IEEE Trans. Ind. Electron.*, Vol. 57, No. 12, pp. 4178-4187, Dec. 2010.

[5] L. Kang, X. Zhao, and J. Ma, "A new neural network model for the state-of-charge estimation in the battery degradation process," *Applied Energy*, Vol. 121, pp. 20-27, May 2014.

[6] Q.-S. Shi, C.-H. Zhang, and N.-X. Cui, "Estimation of battery state-of-charge using ν-support vector regression algorithm," *International Journal of Automotive Technology*, Vol. 9, No. 6, pp. 759-764, Dec. 2008.

[7] G. L. Plett, "Extended Kalman filtering for battery management systems of LiPB-based HEV battery packs: Part 3. State and parameter estimation," *Journal of Power Sources*, Vol. 134, No. 2, pp. 277-292, Aug. 2004.

[8] G. L. Plett, "Sigma-point Kalman filtering for battery management systems of LiPB-based HEV battery packs: Part 1. Introduction and state estimation," *Journal of Power Sources*, Vol. 161, No. 2, pp. 1356-1368, Oct. 2006.

[9] G. L. Plett, "Sigma-point Kalman filtering for battery management systems of LiPB-based HEV battery packs: Part 2: Simultaneous state and parameter estimation," *Journal of Power Sources*, Vol. 161, No. 2, pp. 1369-1384, Oct. 2006.

[10] K. Wei and Q. Chen, "States estimation of Li-ion power batteries based on adaptive unscented Kalman filters," *Proceedings of the CSEE*, Vol. 34, No. 3, pp. 445-452, Jan. 2014.

[11] C. Unterrieder, M. Lunglmayr, S. Marsili, and M. Huemer, "Battery state-of-charge estimation prototype using EMF voltage prediction," in *IEEE International Symposium on Circuits and Systems(ISCAS)*, pp. 622-625, Jun. 2014.

[12] W. Waag and D. U. Sauer, "Adaptive estimation of the electromotive force of the lithium-ion battery after current interruption for an accurate state-of-charge and capacity determination," *Applied Energy*, Vol. 111, pp. 416-427, Nov. 2013.

[13] C. Ehret, S. Piller, W. Schroer, and A. Jossen, "State-of-charge determination for lead-acid batteries in PV-applications," in *Proceedings of the 16th European Photovoltaic Solar Energy Conference*, pp. 1125-1132, 2000.

[14] J. H. Jang and J. Y. Yoo, "Impedance-based and circuit-parameter-based battery models for HEV power systems," *International Journal of Automotive Technology*, Vol. 9, No. 5, pp. 615-623, Oct. 2008.

[15] I.-S. Kim, "The novel state of charge estimation method for lithium battery using sliding mode observer," *Journal of Power Sources*, Vol. 163, No. 1, pp. 584-690, Dec. 2006.

[16] F. Zhang, G. Liu, and L. Fang, "A battery state of charge estimation method using sliding mode observer," in *Proceedings of the 7th World Congress on Intelligent Control and Automation(WCICA)*, pp. 989-994, Jun. 2008.

[17] I. S. Kim, "A technique for estimating the state of health of lithium batteries through a dual-sliding-mode observer," *IEEE Trans. Power Electron.*, Vol. 25, No. 4, pp. 1013-1022, Apr. 2010.

[18] I. S. Kim, "Nonlinear state of charge estimator for hybrid electric vehicle battery," *IEEE Trans. Power Electron.*, Vol. 23, No. 4, pp. 2027-2034, Jul. 2008.

[19] U. Christoph, R. Priewasser, S. Marsili, and M. Huemer, "Battery state estimation using mixed Kalman/H∞, adaptive luenberger and sliding mode observer," in *IEEE Vehicle Power and Propulsion Conference (VPPC)*, pp. 1-6, Oct. 2013.

[20] D. Kim, K. Koo, J. J. Jeong, T. Goh, and S. W. Kim, "Second-order discrete-time sliding mode observer for state of charge determination based on a dynamic resistance li-ion battery model," *Energies*, Vol. 6, No. 10, pp. 5538-5551, Oct. 2013.

[21] B. Pattipati, B. Balasingam, G. V. Avvari, K. R. Pattipati, and Y. Bar-Shalom, "Open circuit voltage characterization of lithium-ion batteries," *Journal of Power Sources*, Vol. 269, pp. 317-333, Dec. 2014.

[22] S. Bao, Y. Feng, and L. Sun, "Robust sliding mode observer design of nonlinear uncertain systems," *Journal of Harbin Institute of Technology*, Vol. 36, No. 5, pp. 613-616, May 2004.

[23] N. Zhang, Y. Feng, and D. Qiu, "Robust sliding mode observer design of nonlinear uncertain systems," *Control Theory & Applications*, Vol. 24, No. 5, pp. 715-718, Oct. 2007.

Qiaoyan Chen was born in Hebei Province, China. He received his M.S. degree in Electrical Engineering from Hebei University of Technology, Tianjin, China, in 2008; and his Ph.D. degree in Control Science and Engineering form Tianjin University, Tianjin, China, in 2014. He is presently a post-doctoral scholar in the School of Electrical Engineering, Beijing Jiaotong University, Beijing, China. His current research interests include battery state estimation, battery management systems, and the design and application of nonlinear observers.

Jiuchun Jiang was born in Jilin Province, China. He received his B.S. degree in Electrical Engineering and his Ph.D. degree in Power System Automation from Northern Jiaotong University, Beijing, China, in 1993 and 1999, respectively. He is presently working as a Professor with the School of Electrical Engineering, Beijing Jiaotong University, Beijing, China. His current research interests include battery application technologies, electric car charging stations and micro-grid technology. He received a National Science and Technology Progress 2nd Award for his work on EV Bus systems, and a Beijing Science and Technology Progress 2nd Award for his work on EV charging systems.

Sijia Liu was born in Henan Province, China. He received his B.S. degree in Electrical Engineering from Beijing Jiaotong University, Beijing, China, in 2013; where he is presently working toward his Ph.D. degree. He is presently with the National Active Distribution Network Technology Research Center, Beijing Jiaotong University. His current research interests include battery modeling, state estimation, and battery management systems.

Caiping Zhang (M'13-SM'14) was born in Henan Province, China. She received her B.S. degree in Vehicular Engineering from the Henan University of Science and Technology, Luoyang, China, in 2004, and her Ph.D. degree in Vehicle Engineering from the Beijing Institute of Technology, Beijing, China, in 2010. From 2010 to 2012, she was a post-doctoral scholar at Beijing Jiaotong University, Beijing, China. She is presently working as an Associate Professor of Beijing Jiaotong University. Her current research interests include battery modeling, states estimation, optimal charging, battery second use technology and battery energy storage systems.